Mg II h+k Flux - Rotational Period Correlation for G-type stars

Manuel Olmedo, Miguel Chávez, Emanuele Bertone, Víctor De la Luz

Instituto Nacional de Astrofísica Optica y Electrónica

Luis Enrique Erro #1 C.P. 72840, Tonatzintla, Puebla, México

olmedo@inaoep.mx, mchavez@inaoep.mx, ebertone@inaoep.mx, itztli@gmail.com

ABSTRACT

We present an analysis of the correlation between the mid-UV Mg II h and k emission lines and measured rotational periods of G-type stars. Based on IUE and HST high resolution spectra of a sample of 36 stars, we derive an exponential function that best represents the correlation. We find that the variation of the Mg II h + k fluxes is about a factor of 2.5 larger than that of Ca II H+K, indicating that the UV features are more sensitive to the decline of $P_{\rm rot}$. The comparison of UV-predicted rotational periods with those derived from empirical $P_{\rm rot}$ - Ca II H+K flux calibrations are consistent, with some scatter at large periods, where the emission are less intense. We present newly derived rotational periods for 15 G-type stars.

Subject headings: Stellar activity, stellar rotation

1. Introduction

The rate at which main sequence stars rotate is certainly amongst the most fundamental stellar parameters. It has proven to be a fundamental tool in a variety of stellar astrophysical phenomena, in particular as a test of the dynamo theories. In the time domain, rotational periods are fundamental for understanding the evolution of angular momentum in low mass stars, from the T-Tauri stage to mature objects as our Sun. Additionally, rotational velocity has become a leading tool for determining stellar ages of main sequence stars in the field, for which other methods, such as the isochrone fitting, are difficult to apply (Soderblom 2010).

Direct measurements of the stellar rotational periods rely on the analysis of brightness variations on the stellar surface due to the presence of spots. Nevertheless, aside from highly magnetic objects of early-type where the spot coverage can be large, this method represents, in many instances, a difficult task for cooler stars. In G-type stars the flux fluctuation is rather weak and requires very long and precise photometric and spectroscopic observational programs. In order to cope with these potential constraints, other in-

direct methods have been implemented, mainly through the analysis of the rotationally driven chromospheric activity.

The correlation between the stellar chromospheric activity and rotation was first identified in the pioneering work of Kraft (1967). This relationship is generally explained by the balance between an enhanced magnetic field induced by rotation and the breaking due to loss of angular momentum by magnetized stellar winds (Mestel 1968). An additional part of the picture is given by the internal magnetic fields generated in the interiors of convective stars ($T_{\rm eff} < 8000$ K) through a solar-like dynamo mechanism.

Magnetic activity has been usually measured by the emission excess in the strong Ca II H and K features. The cardinal work initiated at Mount Wilson in the early sixties (Wilson 1963) was later continued through a number of extensive surveys (see, for instance, Duncan et al. 1991; Henry et al. 1996; Wright et al. 2004; Jenkins et al. 2008; Zhao et al. 2013)

Whilst the Ca II H and K lines have long been the workhorse for stellar activity studies, in particular due to their accessibility from ground based telescopes, the Mg II h and k emission lines in

the mid-UV (2800 Å) has provided an additional valuable diagnostics. These lines, with a similar energetics as those of Ca II, present the advantage that their shallower absorption wings make the emission line easier to measure and less contaminated by the photosphere.

Early works on the Mg II h and k resonance lines by Hartmann et al. (1984) demonstrated that this chromospheric proxy strongly correlates with rotational period, $P_{\rm rot}$. Their study was based on a relatively small sample (31 objects) covering a wide range of mass and evolutionary status, and also included numerous binaries. More recently, Cardini & Cassatella (2007, hereafter CC07) analyzed a larger stellar sample and identified a loose correlation between Mg II flux and rotational period, a situation that is improved if age instead of rotational period is used.

In this paper, we revisit the Mg II h and k doublet as a powerful diagnostics of the rotational period of G-type stars by analyzing a stellar sample of main sequence and subgiant stars observed by International Ultraviolet Explorer (IUE), complemented with high resolution observations conducted by the Space Telescope Imaging Spectrograph (STIS) and the Goddard High Resolution Spectra (GHRS) on board the Hubble Space Telescope (HST). We calibrate the Mg II h and k absolute fluxes with measured rotational periods and apply the relation to determine new rotational periods for 15 stars with high quality UV spectra.

2. The Stellar Sample

The stellar sample upon which our analysis is based has been constructed from two different databases. The first is that of the IUE-Newly Extracted Spectra (INES[1]): we searched for all high resolution data available for objects in class 44 (G-type stars of luminosity classes IV and V). This search delivered nearly 500 spectra that were subsequently visually inspected to verify their quality. A total of 57 objects have been selected from this database. We have also searched available data of G-type stars from HST and found 19 objects, 17 are from STIS, 1 from GHRS, and 1 object have 1 image from both instruments; these data were

taken from the HST-MAST archive[2] and StarCat (Ayres 2010). For the solar spectra, we extracted a high resolution spectrum of the Moon listed in class 02 of the INES archive.

The full sample consists of 75 object plus the Sun. The stellar set is divided into three working sub-samples. The first sub-sample consist of 37 stars (and the Sun) with rotational periods, that we call *primary*, and will be used to establish the calibration of the Mg II UV fluxes vs. rotational period. For these objects, the rotational periods have been measured either through the analysis of the photometric modulation of the visible flux due to the uneven distribution of stellar spots on the stellar surface or through variability of the Ca II emission. The data for these stars are given in Table 1 where columns 1-7 provide, respectively, the star name, the spectral type, the color index $B - V$, the effective temperature mainly obtained from the compilation of Soubiran et al. (2010), the calculated Mg II absolute flux (see next section), the rotational period, and a label of the reference for the period. The list of reference is given at the bottom of the table. The second sub-sample is composed of 23 objects with *secondary* rotational periods, this is, periods determined through a calibration of Ca II emission and measured rotational periods. This dataset will serve as a test to compare rotational periods derived with our UV calibration with those computed from Ca II. Table 2 lists the objects included in this set. Column 1-5 are as in Table 1, while the last 3 columns provide the secondary rotational period, the reference for this period, and the rotational period estimated in this work, respectively. Finally, the third collection corresponds to 15 stars with no available information on their rotational periods, and for which we derive the first estimate of this parameter. This latter set is presented in Table 3, where we also provide our rotational periods and their estimated errors.

3. Measuring the $F_{\rm h+k}$

For the full stellar sample, we have adopted the process described in Hartmann et al. (1984) to measure the observed Mg II h and k fluxes $f_{\rm h+k}$ as the flux integral between the two minima in the h ($h1v, h1r$) and k ($k1v, k1r$) lines from the zero flux

---

[1]http://ines.ts.astro.it/cgi-ines/IUEdbsMY

[2]http://archive.stsci.edu/hst/

Table 1: Basic data for stars with primary rotational periods

Star	Spectral Type	$B-V$	T_{eff} [K]	$\log F_{\text{h+k}}$	P_{rot} [days]	Ref.
Sun	G2V	0.65	5775	6.02	26.09	a
HD1835	G3V	0.67	5776	6.47	7.78	a
HD9562	G1V	0.603	5849	5.68	29	b
HD10700	G8.5V	0.72	5328	5.72	34	b
HD11131	G1Vk:	0.632	5767	6.47	8.92	z
HD13974	G0V	0.58	5606	6.29	11.1	l
HD20630	G5Vv	0.66	5696	6.50	9.24	a
HD25680	G5V	0.62	5867	6.44	9.1	l
HD26756	G5V	0.706	5617	6.50	9.5	j
HD26913	G8V	0.66	5616	6.55	7.15	a
HD27406	G0V	0.572	6200	6.79	5.44	g
HD28034	G0	0.555	6146	6.65	5.2	j
HD28068	G1V	0.62	5758	6.64	7.73	g
HD28205	G0	0.545	6244	6.58	6.7	j
HD28344	G2V	0.619	5898	6.57	7.41	g
HD28805	G5	0.755	5480	6.43	9.04	g
HD30495	G1.5VCH-0.5	0.64	5836	6.51	11	b
HD72905	G1.5Vb	0.58	5863	6.72	4.69	a
HD73350	G5V	0.669	5779	6.44	6.14	z
HD76151	G3V	0.67	5762	6.16	15	b
HD95128	G1V	0.62	5869	5.74	22.7	k
HD97334	G0V	0.61	5850	6.64	7.6	p
HD101501	G8V	0.73	5450	6.29	16.68	a
HD103095	G8Vp	0.75	5055	5.61	31	b
HD114710	G0V	0.58	5963	6.34	12.35	a
HD115383	G0V	0.59	6009	6.66	3.33	a
HD115617	G7V	0.70	5558	5.81	29	b
HD116956	G9V	0.81	5355	6.48	7.8	z
HD117176	G5V	0.71	5530	5.55	31	s
HD128987	G8Vk:	0.737	5557	6.49	9.35	z
HD129333	G1.5V	0.59	5845	6.89	2.8	a
HD142361	G3V	0.64	5175	6.90	1.06	h
HD143761	G0V	0.60	5806	5.84	19	s
HD152391	G8.5Vk:	0.76	5467	6.54	11.43	a
HD182572	G8IV...	0.77	5595	5.85	41	b
HD217014	G2.5IVa	0.70	5760	5.56	37	b
HD283572	G5IV	0.81	4949	6.65	1.55	n
HD131156A	G8V	0.777	5465	6.45	6.16	l

References: (a) Donahue et al. (1996); (b) Baliunas et al. (1996); (g) Pizzolato et al. (2003); (h) Meyer et al. (2006); (j) Duncan et al. (1984); (k) Simpson et al. (2010); (l) Simon & Fekel (1987); (n) Strassmeier (2009); (p) Noyes et al. (1984); (r) Messina (2001); (s) Henry et al. (2000); (z) Gaidos et al. (2000).
Notes: Flux is in units of $[\text{erg} \cdot \text{s}^{-1} \text{cm}^{-2}]$.

level (see Fig. 1). This process was conducted automatically, but verified (and corrected if needed) visually, in particular for stars with lower signal-to-noise in these minima. This method differs from those implemented by Blanco et al. (1974), Linsky & Ayres (1978), and CC07 in that these works either include a correction for the photo-

spheric contribution or perform the integration by considering a local continuum defined by the $k1$ and $h1$ minima. An alternative way to carry out the integration was provided by Buccino & Mauas (2008) who considered a fixed 1.7 Å-width windows to calculate the flux in the k and h lines. In an ideal scenario one should eliminate the photospheric contribution by properly modeling the atmospheric absorption. Nevertheless, the space ultraviolet and in particular the Mg II features in the mid-UV still represent a challenge when modeling stellar atmospheres (see, e.g., Chavez et al. 2007). Additionally, it was argued by Hartmann et al. (1984) that the photospheric contribution in the Mg II lines is much less than for Ca II. Many objects have numerous spectra available, as many as 120 for the case of the star HD2151. For these objects we obtained the mean spectrum by weighting the available spectra by their quoted flux errors.
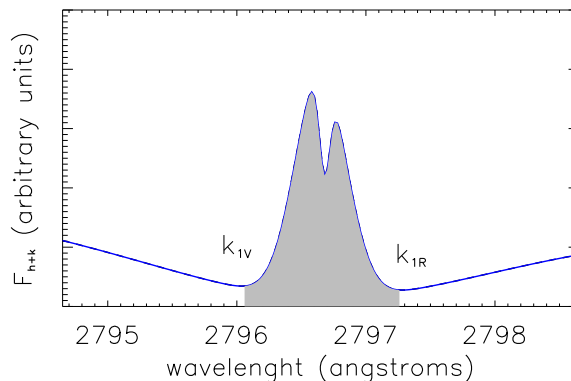

Fig. 1.— Synthetic profile of Mg II k line. The flux integration is made through the $k1v$ and $k1r$ minima limits.

Observed integrated fluxes were then converted to absolute fluxes, F_{h+k}, following the relation of Oranje et al. (1982):

$$\log(F_{\text{h+k}}/f_{h+k}) = 0.328 + 4\log T_{\text{eff}} + 0.4(V + BC). \tag{1}$$

For each object we collected the V magnitudes from SIMBAD database, while the bolometric corrections were taken from Flower (1996). Effective temperatures are mainly from Soubiran et al. (2010) and, for a few objects, from Ammons et al. (2006). In the case of Sun, we have used the IUE

spectrum of the Moon LWR09968HS, which was selected among the 21 available spectra, because of its high quality. For the purposes of treating this spectrum in a similar way as the rest of the stars, we have calculated F_{h+k} by adopting the V magnitude of the solar analog HD102365, a G2V star with stellar parameters very close to solar: $(T_{\rm eff}/\log g/[{\rm Fe/H}])=(5637/4.45/-0.08)$ (Gratton et al. 1996). To obtain the error in the surface flux, we applied a Gaussian error propagation through eq. 1. For the effective temperature, we have used the errors provided in Soubiran et al. (2010) and Ammons et al. (2006) catalogs; for stars with no quoted error in the catalogs, we adopted the mean uncertainty (95 K) of stars with temperature errors available. We assumed for V and BC the conservative values of 1% and 10% relative errors, respectively. The uncertainty on the observed flux f_{h+k} is obtained from the IUE and HST error vectors as a function of the wavelength; we added in quadrature the mean error in the intervals used to integrate each pair of Mg II lines. The latter is the main source of error on F_{h+k}.

In order to test the consistency of our derived fluxes we compare in Fig. 2 our measurements of the Mg II k line flux with those reported by Cardini (2005) (for the 23 objects in common). Whilst the correlation is clear, our fluxes are higher by approximately 25% (about 0.1 dex) on average. This excess can be plausibly explained by the different integration processes. Since Cardini (2005) did not report the IUE images that were used, it is possible that they not coincide with ours, as can be the case of HD2151 for which our flux is 80% larger.

4. The $F_{h+k} - P_{\rm rot}$ Correlation

In the upper panel of Fig. 3 we plot F_{h+k} vs. the rotational periods for the 38 objects (including the Sun) which have primary values for their rotational periods (Table 1). In this plot the different symbols stand for the origin of the data as indicated in the panel. All stars correspond to luminosity classes objects V except for the squared symbol that shows the location of the only luminosity class IV star. The starred symbol indicates the position of the Sun. We have attempted several functional forms to calculate the best fit and
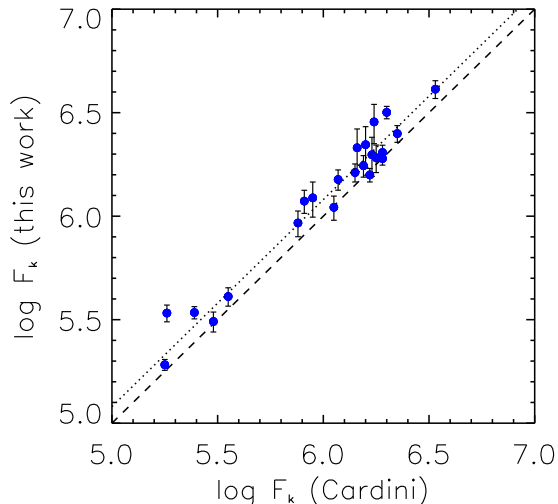

Fig. 2.— The absolute flux for the Mg II k line ($F_{\rm k}$) measured in this work vs. those of Cardini (2005). The dashed line is the one-to-one relation and the dotted line is a linear fit to the data. A similar procedure is used for the Mg II h line.

found that the function:

$$\log F_{h+k} = A + Be^{\log P_{\rm rot}/C}. \qquad (2)$$

where the coefficient $A = 7.125, B = -0.162, C = 0.674$ provided the lowest χ^2. The function is compatible with the exponential used in Noyes et al. (1984). However, as in Noyes et al. (1984), the adopted functional form does not have physical implications.

There is a relatively tight correlation for our sample of G-type stars, with much less dispersion than that observed in other works (e.g. Hartmann et al. 1984; Cardini & Cassatella 2007), that can be explained by the exclusion of the more active cool K and M-type stars. The lines in the plot correspond to the best fitted exponential function (solid line) and the $\pm 1\sigma$ levels (dashed lines).

Whilst at low rotational periods ($P_{\rm rot} < 4$d) the diagram is less populated, the correlation indicates that for $P_{\rm rot} = 0$ the flux appears to reach a maximum of $\log F_{h+k} \sim 6.8$. For periods larger than 4 days there is a decline of more than one decade. The three stars indicated with
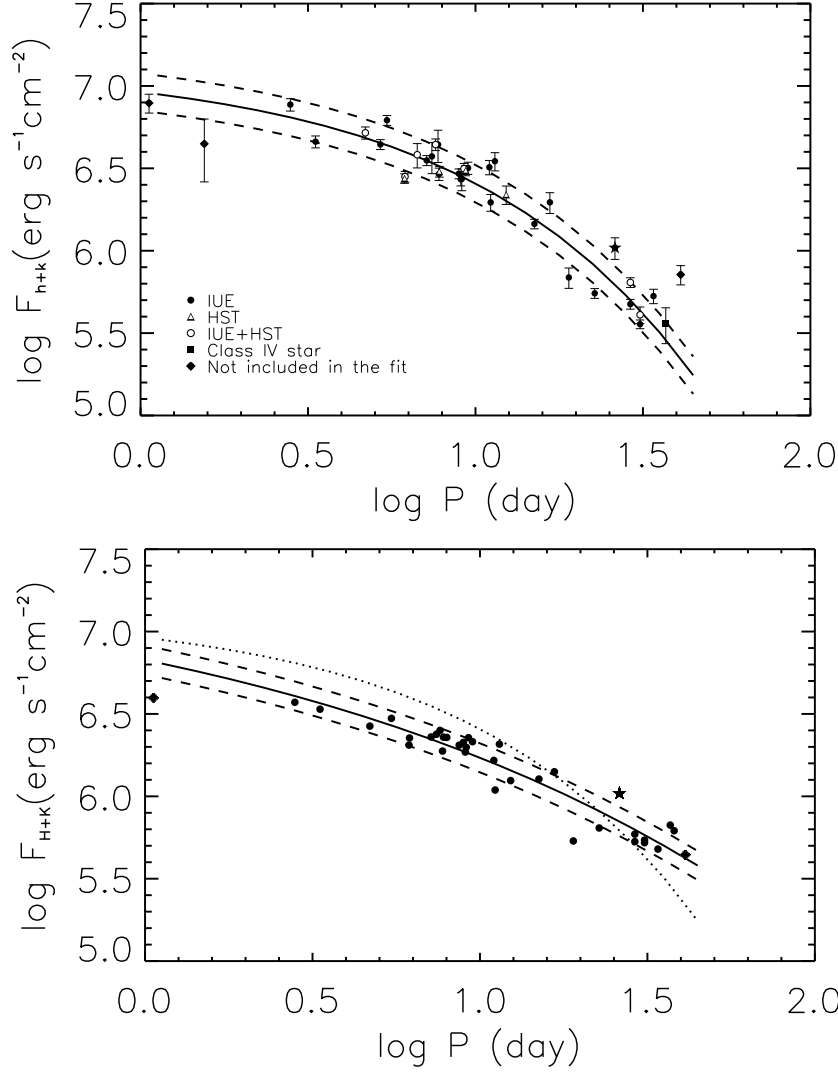
Fig. 3.— Top panel: Mean Mg II h+k flux (F_{h+k}) as function of rotational period. Solid circles, open circles and open triangles are mean F_{h+k} from IUE, HST, and HTS+IUE spectra, respectively. The sun is indicated with a star. The solid line is the best fit to the data, while the dashed lines indicate the ± 1 sigma error. Diamonds are stars not used in the fit. Bottom Panel: Ca II H+K flux vs. rotational period, F_{H+K} derived from the R_{H+K} values given by Henry et al. (1996) and Wright et al. (2004). The solid line is the best fit using a similar exponential function as for UV data, shown as a dotted line.

diamonds were not taken into account in the fitting calculation. The two with the lowest rotational periods correspond to pre-main sequence objects, whose inclusion would produce, in any case, negligible changes in the fitted function.

The other object, which shows the largest deviation from the correlation depicted in Fig. 3, is the metal-rich star HD182572. This a G8IV variable star whose rotational period of 41 days ($\log P_{\rm rot} = 1.61$, Baliunas et al. 1996) appears to

5

be twice as large as predicted by its Mg II flux. Its measured rotational period is compatible with the period of $\sim$37 days estimated from the average rotational velocity ($v \sin i$) of 1.9 km s^{-1} in Glebocki & Gnacinski (2005) and the stellar radius of $1.38 R_\odot$ (Boyajian et al. 2013). Variability can be a possible explanation for the discrepancy, however, Lockwood et al. (1997) found the root mean square of the brightness variation in Strömgren b and y bands to be just 0.0016 mag during a 12-year long interval (1984-1995). It is possible that an enhanced activity epoch around the IUE observation date (December 1979) produced such a strong UV flux, although this scenario might not be supported by the Ca II S-index monitoring by Duncan et al. (1991), unless the IUE observation actually coincided with a transient event.

An important aspect of the observed correlation of Mg II vs. $P_{\rm rot}$ is the range of variation of $\log F_{\rm h+k}$. The difference between the highest and lowest values is 1.60 dex. In order to compare this difference with that to be expected from Ca II measurements, we have used the available $R_{\rm H+K}$ fluxes for the calcium line from Henry et al. (1996) and Wright et al. (2004) for the stars of our sample and transformed them into $F_{\rm H+K}$ by multiplying $R_{\rm H+K}$ by the bolometric luminosity σT^4, according to the definition of Noyes et al. (1984). We fit a similar function to eq. 2 to the $F_{\rm H+K} - P_{\rm rot}$ values; this is shown in the lower panel of Fig. 3, where the dotted line is the fit for Mg II case. Note that the variation of $F_{\rm H+K}$ is 1.20 dex, i.e. about 0.4 dex smaller than that for Mg II. We would like to remark that, should we have included the star with the lowest rotational period (HD142361) the Ca II flux variation would have decreased to 1.09 dex due to the steeper correlation in the low period edge.

Another interesting feature of the panels depicted in fig. 3 is that the average standard deviation for both correlations are quite similar, with that of Mg II ($\sigma_{\rm h+k} \sim 0.11$ dex) slightly larger than for Ca II (~ 0.09 dex). In this regard, we have conducted a simple test to understand the extent to which the standard deviation can be ascribed to the $F_{\rm h+k}$ intrinsic variability of each star. For this purpose, we have compared the amplitude of the variation of the flux in the Mg II lines, $\Delta \log F_{\rm h+k}$, with $\sigma_{\rm h+k}$, for the 17 stars with multiple observations. The results of such a comparison indicate that $\Delta \log F_{\rm h+k} < \sigma_{\rm h+k}$ in 15 out of 17 cases. The main results of the analysis presented above demonstrates that the magnesium index is about 2.5 times more sensitive to rotational period than that of calcium.

5. New Rotational Periods

A direct application of the exponential fit obtained in the previous section is the determination of new rotational periods ($P_{\rm rot3}$) for the objects in Table 3. It is, however, important to compare UV derived periods with those determined from secondary methods, mainly through the calibration of the Ca II H and K lines. For this purpose we use the second stellar set in Table 2, for which we have collected calculated rotational periods from the literature: these secondary rotational periods ($P_{\rm rot2}$) are mainly from Soderblom (1985), Wright et al. (2004), and a few from Baliunas et al. (1996) and Saar & Osten (1997). In Fig. 4 we illustrate the comparison of the Mg II vs Ca II rotational periods. The dashed line correspond to slope unity.

In general the points cluster around the one-to-one correlation with less agreement at large rotations periods ($P_{\rm rot} > 20$d), hence for more mature stars with less intense chromospheric emission. The point that most deviate from the correlation is that for star HD188512 (βAql, for which derive $P_{\rm rot} = 35.1$d significantly smaller than the Ca II derived periods in excess of 50 days. This star is a subgiant star which has 15 determinations of atmospheric parameters in the compilation of Soubiran et al. (2010). The effective temperatures for this object range from 4373 K to 5478 K, surface gravities from 1.3 dex to 3.79 dex and a metallicity whose determinations vary nearly 0.6 dex. Even if we exclude the lowest gravity and highest temperature values (Luck & Heiter 2006; Luck & Lambert 1981)[3], this star has averaged parameters that are discrepant with the rest of the luminosity class IV stars in our sample, in particular for gravity. Being a more evolved star,

---

[3] We would like to point out that there is a probable identification mismatch. According to Soubiran et al. (2010), the lowest value of $\log g$ for HD188512 has been compiled from Luck & Lambert (1981), however, this latter study is for supergiant stars, and the one with the reported parameters actually is β Aqr, a G0Ib star.
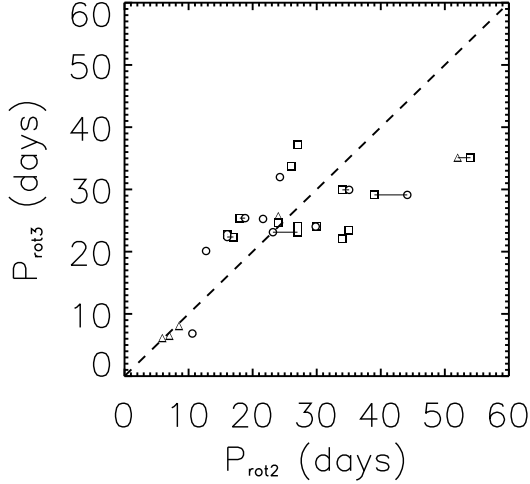
Fig. 4.— Comparison of calculated rotational periods ($P_{\rm rot3}$) and secondary rotational periods from literature ($P_{\rm rot2}$). Squares and circles have rotational periods from Wright et al. (2004) and Soderblom (1985), respectively, triangles are from Baliunas et al. (1996) or Saar & Osten (1997). Stars with periods from both groups are connected.

the correlation given by eq. 2 is most probably not applicable to this object.

For the stars in Table 3 we provide for the first time an estimation of their rotational period (column 6) and their uncertainties (column 7). Errors have been obtained through Gaussian propagation of errors of the fitting parameters of eq. 2. Rotational periods for this sample span a wide range of values, from $P_{\rm rot} = 2.7$d for HD212697 to 35.8d for HD212330. There are several objects with $P_{\rm rot}$ very similar to that of the Sun.

Table 2: Basic data for stars with secondary rotational periods

Star	Spectral Type	$B-V$	$T_{\rm eff}$ [K]	$\log F_{\rm h+k}$	$P_{\rm rot2}$ [days]	Ref.	$P_{\rm rot3}$ [days]	$\sigma_{P_{\rm rot3}}$ [days]
HD26923	G0IV	0.56	5986	6.58	7	c	6.5	1.7
HD30649	G1V-VI	0.58	5791	5.92	17	w	22.4	1.7
HD34411	G1.5IV-V	0.64	5821	5.61	24	i	32.0	1.8
HD43587	G0V	0.59	5899	5.82	22	i	25.3	1.7
HD52711	G4V	0.60	5891	5.82	18	w	25.4	1.7
HD67228	G1IV	0.60	5738	5.45	27	w	37.2	1.8
HD84737	G0.5Va	0.61	5894	5.89	27	w	23.1	1.8
HD101563	G0V	0.66	5902	5.86	27	w	24.0	1.7
HD102365	G2V	0.66	5575	5.81	24	d	25.7	1.7
HD104304	G8IV	0.78	5542	5.88	35	w	23.5	1.7
HD109358	G0V	0.60	5901	5.91	16	w	22.8	1.8
HD110897	G0V	0.50	5863	6.00	13	i	20.1	1.7
HD120066	G0.5IV-V	0.66	5923	5.56	26	w	33.7	1.8
HD144579	G8V	0.73	5301	5.67	34	w	29.9	1.7
HD146233	G2Va	0.65	5785	5.84	24	w	24.7	1.7
HD147513	G5V	0.60	5850	6.50	8.5	d	8.1	1.7
HD150706	G3V	0.57	5918	6.56	11	i	6.8	1.9
HD157214	G0V	0.61	5675	5.86	30	i	24.0	1.7
HD157347	G5IV	0.65	5677	5.86	30	w	24.1	1.7
HD165185	G1V	0.57	5854	6.60	6	d	6.1	1.7
HD182488	G8V	0.79	5421	5.70	39	w	29.1	1.8
HD188376	G5IV	0.75	5505	5.93	34	w	22.1	1.7
HD188512	G9.5IV	0.85	5091	5.52	54	w	35.1	1.8

References: (c) Baliunas et al. (1996); (d) Saar & Osten (1997); (i) Soderblom (1985); (w) Wright et al. (2004).
Notes: Flux is in units of $[\rm erg \cdot s^{-1} cm^{-2}]$.

Table 3: Stars with newly determined rotational periods

Star	Spectral Type	$B-V$	$T_{\rm eff}$ [K]	$\log F_{\rm h+k}$ $[\rm erg \cdot s^{-1} cm^{-2}]$	$P_{\rm rot3}$ [days]	$\sigma_{P_{\rm rot}}$ [days]
HD2151	G0V	0.62	5773	5.76	27.1	1.7
HD16417	G1V	0.67	5797	5.82	25.2	1.7
HD20794	G8V	0.71	5430	5.80	25.9	1.7
HD44594	G1.5V	0.65	5799	5.96	21.2	1.7
HD59967	G3V	0.64	5780	6.56	7.00	1.7
HD76932	G2V	0.53	5849	5.94	21.9	1.7
HD136352	G4V	0.63	5623	5.78	26.7	1.7
HD181321	G2V	0.59	5816	6.63	5.7	1.7
HD184499	G0V	0.59	5723	5.98	20.7	1.7
HD190248	G8IV	0.76	5544	5.61	31.9	1.7
HD196378	G0V	0.51	6038	5.74	27.7	1.7
HD203244	G5V	0.73	5525	6.50	8.1	1.7
HD212330	G2IV-V	0.68	5650	5.50	35.8	1.8
HD212697	G3V	0.71	5769	6.82	2.7	1.9
HD225239	G2V	0.64	5593	5.90	22.9	1.7

6. Summary

We have measured the flux of the mid-UV emission lines Mg II h and k for 76 stars G-type stars (including the Sun) in the main sequence or in the subgiant branch. We used the 38 objects with a rotational period obtained from the periodic variability of their light curves to derive an analytical calibration of F_{h+k} vs. P_{rot}. We found a tight correlation, which benefits from the inclusion of HST observations as they have a significantly better signal-to-noise ratio compared to the IUE spectra. This is the first time that HST UV data are used in the analysis of this relation, which we used to obtain the first estimates of the rotational periods for 15 stars with high quality mid-UV data.

Our results indicate that the Mg II h and k lines are about 2.5 times more sensitive to the rotational period than the frequently used chromospheric proxy of Ca II. The comparison of our UV-derived rotational periods with those obtained from similar correlations for Ca II shows a significant scatter for slow rotator, where perhaps the very faint Ca II H and K emission might be prone to large uncertainties.

APPENDIX A

Identification of IUE and HST images

Table 4: Image identification of some of the spectra used in this work. The full list is available upon request from the authors

Star	fits name
SUN	LWR09968HS_2790_2810
HD001835	LWP21832HL_2790_2810
	LWR11867HL_2790_2810
	LWP21823HL_2790_2810
	LWP14463HL_2790_2810
	LWR11851HL_2790_2810
	LWP24326HL_2790_2810
	LWP22038HL_2790_2810
	LWP22037HL_2790_2810
	LWP22005HL_2790_2810
	LWP22004HL_2790_2810
	LWP23657HL_2790_2810
HD009562	LWP02200HL_2790_2810
HD010700	LWR03702HL_2790_2810
	LWP04912HL_2790_2810
	LWR11587HL_2790_2810
	LWP02224HL_2790_2810
	LWR13817HL_2790_2810
	LWR04958HL_2790_2810
HD011131	LWP03613HL_2790_2810

REFERENCES

Ammons, S. M., Robinson, S. E., Strader, J., et al. 2006, ApJ, 638, 1004

Ayres, T. R. 2010, ApJS, 187, 149

Baliunas, S., Sokoloff, D., & Soon, W. 1996, ApJ, 457, L99

Blanco, C., Catalano, S., Marilli, E., & Rodonò, M. 1974, A&A, 33, 257

Boyajian, T. S., von Braun, K., van Belle, G., et al. 2013, ApJ, 771, 40

Buccino, A. P., & Mauas, P. J. D. 2008, A&A, 483, 903

Cardini, D. 2005, A&A, 430, 303

Cardini, D., & Cassatella, A. 2007, ApJ, 666, 393

Chavez, M., Bertone, E., Buzzoni, A., et al. 2007, ApJ, 657, 1046

Donahue, R. A., Saar, S. H., & Baliunas, S. L. 1996, ApJ, 466, 384

Duncan, D. K., Frazer, J., Lanning, H. H., et al. 1984, PASP, 96, 707

Duncan, D. K., Vaughan, A. H., Wilson, O. C., et al. 1991, ApJS, 76, 383

Flower, P. J. 1996, ApJ, 469, 355

Gaidos, E. J., Henry, G. W., & Henry, S. M. 2000, AJ, 120, 1006

Glebocki, R., & Gnacinski, P. 2005, VizieR Online Data Catalog, 3244, 0

Gratton, R. G., Carretta, E., & Castelli, F. 1996, A&A, 314, 191

Hartmann, L., Baliunas, S. L., Noyes, R. W., & Duncan, D. K. 1984, ApJ, 279, 778

Henry, G. W., Baliunas, S. L., Donahue, R. A., Fekel, F. C., & Soon, W. 2000, ApJ, 531, 415

Henry, T. J., Soderblom, D. R., Donahue, R. A., & Baliunas, S. L. 1996, AJ, 111, 439

Jenkins, J. S., Jones, H. R. A., Pavlenko, Y., et al. 2008, A&A, 485, 571

Kraft, R. P. 1967, ApJ, 150, 551

Linsky, J. L., & Ayres, T. R. 1978, ApJ, 220, 619

Lockwood, G. W., Skiff, B. A., & Radick, R. R. 1997, ApJ, 485, 789

Luck, R. E., & Heiter, U. 2006, AJ, 131, 3069

Luck, R. E., & Lambert, D. L. 1981, ApJ, 245, 1018

Messina, S. 2001, A&A, 371, 1024

Mestel, L. 1968, MNRAS, 138, 359

Meyer, M. R., Hillenbrand, L. A., Backman, D., et al. 2006, PASP, 118, 1690

Noyes, R. W., Hartmann, L. W., Baliunas, S. L., Duncan, D. K., & Vaughan, A. H. 1984, ApJ, 279, 763

Oranje, B. J., Zwaan, C., & Middelkoop, F. 1982, A&A, 110, 30

Pizzolato, N., Maggio, A., Micela, G., Sciortino, S., & Ventura, P. 2003, A&A, 397, 147

Saar, S. H., & Osten, R. A. 1997, MNRAS, 284, 803

Simon, T., & Fekel, Jr., F. C. 1987, ApJ, 316, 434

Simpson, E. K., Baliunas, S. L., Henry, G. W., & Watson, C. A. 2010, MNRAS, 408, 1666

Soderblom, D. R. 1985, AJ, 90, 2103

—. 2010, ARA&A, 48, 581

Soubiran, C., Le Campion, J.-F., Cayrel de Strobel, G., & Caillo, A. 2010, A&A, 515, A111

Strassmeier, K. G. 2009, A&A Rev., 17, 251

Wilson, O. C. 1963, ApJ, 138, 832

Wright, J. T., Marcy, G. W., Butler, R. P., & Vogt, S. S. 2004, ApJS, 152, 261

Zhao, J. K., Oswalt, T. D., Zhao, G., et al. 2013, AJ, 145, 140